Modeling of Spatial Distribution of the Piping Hazard for River Dikes Based on Actual Data

Hiroto Koide[1] and Yu Otake[2]

[1]Niigata University, Niigata, Japan.
E-mail: koide-h573bt@pwri.go.jp
[2]Niigata University, Niigata, Japan.
E-mail: y_ohtake@eng.niigata-u.ac.jp

Abstract: In recent years, the failure and large-scale deformation of river dike embankment due to the soil piping phenomenon in permeable foundation ground during floods have frequently been reported in Japan. The soil piping phenomenon arises from the soil layer composition of the foundation ground and is very local for a long river. Previous soil investigations that conduct measurements at intervals of several hundred meters along the river dike embankment in Japan can overlook sites at risk of piping. Therefore, quantification of the interpolation errors between investigation points can help with the rational management of river dike. In this paper, tests of methods for piping risk analysis are conducted by accounting for the interpolation errors between soil investigations. Specifically, we compare three models: simple kriging, a local level model (LL-model), and a local level model considering local levee conditions (LLL-model).

Keywords: State-space model; spatial variability; piping; risk management; river dike.

1 Background and Purpose

In recent years, the failure and large-scale deformation of river dikes due to the soil piping phenomenon in permeable foundation ground during floods have frequently been reported in Japan. Many researchers in geotechnical engineering have conducted in-depth studies to better understand the mechanisms of failure progression and to identify dangerous soil condition. For example, in the Yabe River, the foundation (ground) of the failed section was reported as a combination of sandy (As) and gravel (Ag) soils. Previous studies have suggested that this soil layer combination is likely to lead to failure progression. Therefore, if this soil layer composition is found in prior investigations, effective management can be applied. However, in the case of the Yabe River, the soil layer composition was known to be deposited within several tens of meters along the river. This suggests that modeling the soil layer structure in detail where local changes can be considered is a major problem. Although not only in Japan but also overseas researchers have focused on modeling soil layer composition, these studies usually assume that the prediction of the soil layer structure of river dikes is very difficult since the soil layer is discretely deposited over the long history of the sedimentary environment.

In this study, we consider a method for modeling the spatial variability of the critical water level (m) that leads to piping. We discuss the effectiveness of various methods by quantifying the interpolation error between soil investigations modeled with simple kriging, a local level model (LL-model), and a local level model considering local levee conditions. (LLL-model).

2 Data Used in This Study

2.1 Geological profile of the target river dike (soil investigation data)

For the analysis, we use data from the 35-km extension of the left bank of a fairly large river running through one of the major cities in Japan. Soil investigations were conducted at the target river dike in intervals of approximately 100 to 200 m (the number of bore holes is 75). Furthermore, the longitudinal soil figure has been drawn considering not only the soil investigations but also knowledge from the viewpoint of geological sciences (i.e., the process of terrain formation, information on micro-topographic classification and so on). Assuming that the longitudinal soil figure is true, the map was divided into a mesh with intervals of 0.2 m in the vertical direction and 50 m in the horizontal direction, and the soil classification and layer thicknesses were scanned into digital data (Fig. 1(a)). The data will be referred to as “the soil investigation data” below.

2.2 Environmental condition data of the target river dike (local levee condition)

In addition to these soil investigation data, we gathered continuous data about environmental conditions along the river dike. To distinguish these data from soil investigation data, we refer to such data as “the local levee

Proceedings of the 7th International Symposium on Geotechnical Safety and Risk (ISGSR)
Editors: Jianye Ching, Dian-Qing Li and Jie Zhang

Published by Research Publishing, Singapore.
ISBN: 978-981-11-2725-0; doi:10.3850/978-981-11-2725-0_IS9-18-cd

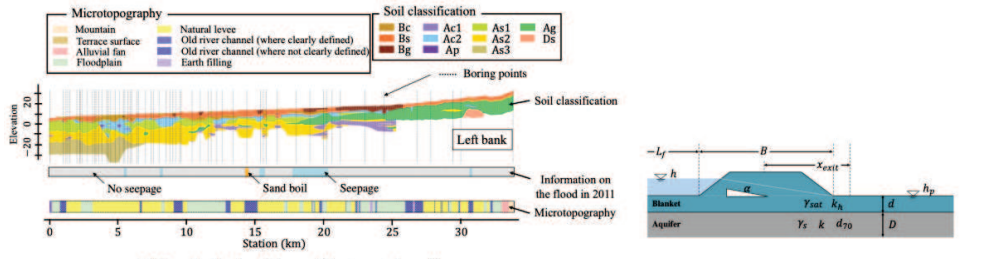

Figure 1. Soil investigation data in the target river dike using calculation

conditions". We measured five local levee conditions at points i, which are denoted as $\mathbf{z}_i = (z_{i,1}, z_{i,2}, \ldots, z_{i,5})^t$, where the superscript "t" denotes the matrix transpose.

$$\mathbf{Z} = \begin{pmatrix} | & | & & | \\ \mathbf{z}_1 & \mathbf{z}_2 & \cdots & \mathbf{z}_N \\ | & | & & | \end{pmatrix} \tag{1}$$

The subscript N in $\mathbf{z}_i$ represents the number of estimated points along the river embankment. The soil investigation data is generally acquired as discrete data, but the local levee conditions can be measured at all points, and the discrete soil investigation data can be interpolated with the continuous local levee condition. The local levee conditions at point i comprise the following data: $z_{i,1}$ is the width of levee B (m), $z_{i,2}$ is the average hydrodynamic gradient of the levee body α (-), $z_{i,3}$ is the thickness of the hinterland blanket d (m), $z_{i,4}$ indicates the variations of medium and small scale flooding in the past (-) (1 : with variations; 0 : no variation), and $z_{i,5}$ is the microtopography (-) (1 : old river channel or natural levee; 0 : the others).

3 Method for This Study

3.1 Calculation procedure

Step-1: Calculation of critical water level for piping.

In step 1, the critical water level for piping h_c (m) of target river is calculated by the method proposed by Schweckendiek (2014). The calculated h_c (m) is assumed a true ("True data").

Step-2: Generation of the "thinning data".

The "True data" in Step-1 is intentionally thinned out to create new data ("Thinning data").

Step-3: Interpolate "Thinning data" with the three proposed models.

3.2 Reliability analysis

This study adopted the procedure for calculating progressive piping failure proposed by Schweckendiek (2014). Schweckendiek (2014) models the progress of the piping phenomenon as a parallel system of three limit states: UPLIFT (rising of the bottom), HEAVE (quicksand), and PIPING (backward erosion piping). Calculations corresponding to each limit state (UPLIFT, HEAVE, and PIPING) are described in closed form, and their reliability has been verified using model experiments at many different scales. Each limit state functions Z_u, Z_h, and Z_p can be considered the cumulative resistance against the main loading on river levees - the water level h as follows.

$$Z_u = g_u(\mathbf{x}) = h_{c,u} - h \tag{2}$$

$$Z_h = g_h(\mathbf{x}) = h_{c,h} - h \tag{3}$$

$$Z_p = g_p(\mathbf{x}) = h_{c,p} - h \tag{4}$$

where $h_{c,u}$, $h_{c,h}$, and $h_{c,p}$ are the critical water levels for UPLIFT, HEAVE, and PIPING, respectively, and h is the water level. To calculate each critical water level ($h_{c,u}$, $h_{c,h}$, $h_{c,p}$), we use Monte Carlo simulation (MCS). The conceptual diagram of embankment shape of the river dike and the statistical values of the calculation parameters used for calculation are shown in Figure 1(b) and Table 1.

Schweckendiek (2014) claimed that embankment failure by piping takes place only when all three limit states—UPLIFT, HEAVE and PIPING—are exceeded. This can be described by a parallel system as follow.

$$F = \left\{ g_u(\mathbf{x}) < 0 \cap g_h(\mathbf{x}) < 0 \cap g_p(\mathbf{x}) < 0 \right\} \tag{5}$$

Hence, the parallel system problem of uplift, heave and piping can be formulated as:

$$F = \{\max[g_u(\mathbf{x}), g_h(\mathbf{x}), g_p(\mathbf{x})] < 0\} \tag{6}$$

Similarly, the critical water level as a parallel system h_c is can be formulated as:

$$h_c = \max[h_{c,u}, h_{c,h}, h_{c,p}] \tag{7}$$

Table 1. Random variables for the calculation procedure

Symbol	Parameter	Unit	Distribution type	Mean	Var	COV	Notes
d	Thickness of the hinterland blanket	m	Deterministic	–	–	–	Depending on location
D	Aquifer thickness	m	Deterministic	–	–	–	Depending on location
B	Width of the levee	m	Deterministic	24.0	–	–	Depending on location
L_f	Length of the foreshore	m	Uniform	–	–	–	$\alpha_u = 0$ $\beta_u = 15.0$
x_{exit}	Distance from the exit point to the center of the levee footprint	m	Uniform	–	–	–	$\alpha_u = B/2$ $\beta_u = B$
γ_{sat}	Saturated volumetric weight of the blanket	kN/m^3	Normal	18.0	3.50^2	0.15	–
γ_w	Volumetric weight of water	kN/m^3	Deterministic	10.0	–	–	–
θ	Bedding angle	deg	Deterministic	37.0	–	–	–
$\log_e(d_{70})$	70% fractile of the grain size distribution	m	Normal	Clay −4.64 Sand −8.04 Gravel −10.77	0.65^2 0.52^2 0.94^2	−0.14 −0.06 −0.09	–
d_{70m}	Reference value for d_{70}	m	Deterministic	2.08×10^{-4}	–	–	–
$\log_{10}(k_h)$	Permeability of the blanket	m/s	Beta	–	–	–	Clay $\alpha_b = 4.96, \beta_b = 3.90$
$\log_{10}(k)$	Permeability of the aquifer	m/s	Beta	–	–	–	Sand $\alpha_b = 3.29, \beta_b = 3.25$ Gravel $\alpha_b = 1.07, \beta_b = 3.43$
h	Water level at the entry point	m	Weibull	–	–	–	Depending on location
h_p	Phreatic level at the exit point	m	Deterministic	–	–	–	Depending on location
η	Drag factor coefficient	–	Deterministic	0.25	–	–	–
υ	Kinematic viscosity of water	m^2/s	Deterministic	1.33×10^{-6}	–	–	–
$i_{c,h}$	Critical levee hydraulic gradient	–	Lognormal	0.70	0.10^2	0.14	–
m_u	Model factor addressing the uncertainty in the critical gradient	–	Lognormal	1.00	0.10^2	0.10	–
m_ϕ	Model factor addressing the uncertainty in the actual gradient	–	Lognormal	1.00	0.10^2	0.10	–
m_p	Model uncertainty factor of piping	–	Lognormal	1.00	0.12^2	0.12	–

3.3 Quantification of interpolation error

We examine the effectiveness of a method for quantifying the risk associated with the statistical estimation error due to lack of soil investigation by interpolating the discrete soil investigation data. The following three analysis methods are compared.

3.3.1 Method 1: Simple Kriging (Bayesian inference)

For interpolation between investigation points, we use the popular method of kriging. Among the various methods proposed for kriging, we use the simple kriging method. The reason for selecting Simple Kriging is that this method is interpreted to be a method of Bayesian inference (Hoshiya 1996). This method can be interpreted as a Bayesian estimation; thus, we chose this kriging method for easy comparison with Methods 2 and 3, wherein a hierarchical Bayesian model is applied.

3.3.2 Method 2: Local level model (hierarchical Bayesian inference with state-space model)

A state-space model is a statistical model in which a time series is expressed by a pair of equations that are called the state equation and the observation equation (Durbin and Koopman 2002, 2012). The local level model (LL-model) that is the simplest for the state-space model is chosen. This model is defined by the following equations.

$$x_i = x_{i-1} + v_i, \qquad v_i \sim N(0, V) \tag{8}$$

$$y_i = x_i + w_i, \qquad w_i \sim N(0, W) \tag{9}$$

Here, Eqs. (8) and (9) are the state equation and observation equation, respectively, and $\mathbf{X}(x_1, x_2, \cdots, x_N)$ is the state vector. The state vector has the dimension of the estimated points of N. $\mathbf{Y}(y_1, y_2, \cdots, y_N)$ is a partially deficient observation vector. We assume that v_i and w_i are state and observation noises, respectively; that they are independent within and between series; and that they conform with the formulas $v_i \sim N(0, V)$ and $w_i \sim N(0, W)$. The $N+2$ unknown parameters comprise the state vectors $\mathbf{X}(x_1, x_2, \cdots, x_T)$ and the variances V and W of the state noise and observation noise. State noise and observation noise are hyperparameters and are expressed as $\boldsymbol{\theta}_1 = (\boldsymbol{V}, \boldsymbol{W})^t$.

The Bayesian estimation method is used for parameter estimation. Assuming the prior distribution of the hyperparameter vector, $p(\boldsymbol{\theta}_1)$, the posterior distribution is defined by the following equation that describes Bayes' theorem.

$$p(\boldsymbol{\theta}_1, \mathbf{X}|\mathbf{Y}) = \frac{p(\mathbf{Y}|\mathbf{X}, \boldsymbol{\theta}_1) p(\mathbf{X}|\boldsymbol{\theta}_1) p(\boldsymbol{\theta}_1)}{p(\mathbf{Y})} = \frac{p(x_0) p(\boldsymbol{\theta}_1) \prod_{i=1}^{N} p(y_i|x_i) p(x_i|x_{i-1}, \boldsymbol{\theta}_1)}{p(\mathbf{Y})} \tag{10}$$

Using Markov chain Monte Carlo (MCMC) modeling, samples are taken from the posterior distribution defined by Eq. (10), and the results are discussed.

3.3.3 Method 3: Local level model considering local levee condition (hierarchical Bayesian inference with state-space model)

The local level model considering local levee condition (LLL-model) is a model that considers local levee condition of the river embankment in Model 2. This model is different from Method 2 (LL-model) in observation equation. We consider to interpolate discrete the soil investigation data by using local levee condition where information. The state and observation equations are as follows.

$$x_i = x_{i-1} + v_i, \qquad v_i \sim N(0, V) \tag{11}$$

$$y_i = x_i + \boldsymbol{\beta}\mathbf{z}_i + w_i, \qquad w_i \sim N(0, W) \tag{12}$$

Here, the new parameters $\boldsymbol{\beta}$ and $\mathbf{z}_i$ are expressed as $\boldsymbol{\beta} = (\beta_1, \cdots, \beta_5)^t$ and $\mathbf{z}_i = \left(z_{i,1}, \ldots, z_{i,5}\right)^t$, respectively, indicating the regression coefficients of the local levee condition and the data of the local levee condition at point i. The observation equation is different from that of the LL-model, and the objective is to correct the spatial distribution characteristics depending on the local levee conditions.

The $N+7$ unknown parameters comprise the state vector $\mathbf{X}$ of the state equation, the variance V of the state noise, the variance $\mathbf{W}$ of the observation noise, and the coefficient vector of the local levee conditions $\boldsymbol{\beta}$. Assuming a new hyperparameter $\boldsymbol{\theta}_2 = (\beta_1, \cdots, \beta_5)^t$, the posterior distribution can be expressed using the following equation.

$$p(\boldsymbol{\theta}_1, \boldsymbol{\theta}_2, \mathbf{X}|\mathbf{Y}) = \frac{p(\mathbf{Y}|\mathbf{X}, \boldsymbol{\theta}_1, \boldsymbol{\theta}_2) p(\mathbf{X}|\boldsymbol{\theta}_1, \boldsymbol{\theta}_2) p(\boldsymbol{\theta}_1) p(\boldsymbol{\theta}_2)}{p(\mathbf{Y})} = \frac{p(x_0) p(\boldsymbol{\theta}_1) p(\boldsymbol{\theta}_2) \prod_{i=1}^{N} p(y_i|x_i) p(x_i|x_{i-1}, \boldsymbol{\theta}_1, \boldsymbol{\theta}_2)}{p(\mathbf{Y})} \tag{13}$$

4 Analysis Result

Figure 2 shows the results of the critical water level and reliability index calculated when it is assumed that the soil investigation is conducted at 200m intervals along the target river. The upper part of Fig. 2 shows the critical water level h_c (m) and the lower part shows the reliability index. The blue line in the upper part shows the median of the critical water level, and the dark-gray shaded area and the light-gray shaded area show the range of 50% and 90% of critical water level, respectively. In this analysis, the median of the critical water level are assumed to be true (True data). The green shaded area in the lower part of Fig. 2 shows the target reliability range defined by ISO.

The next analysis, we verify the effectiveness of each model by preparing data that was intentionally thinned out from the true data (Thinning data) and comparing the interpolation result using the thinning data with the true data.

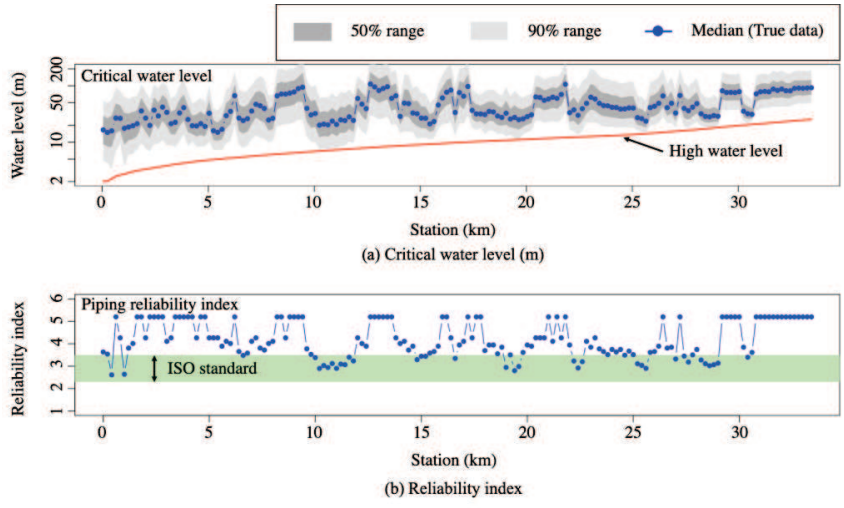

Figure 2. Reliability analysis results assuming to be conducted soil investigation at 200m intervals

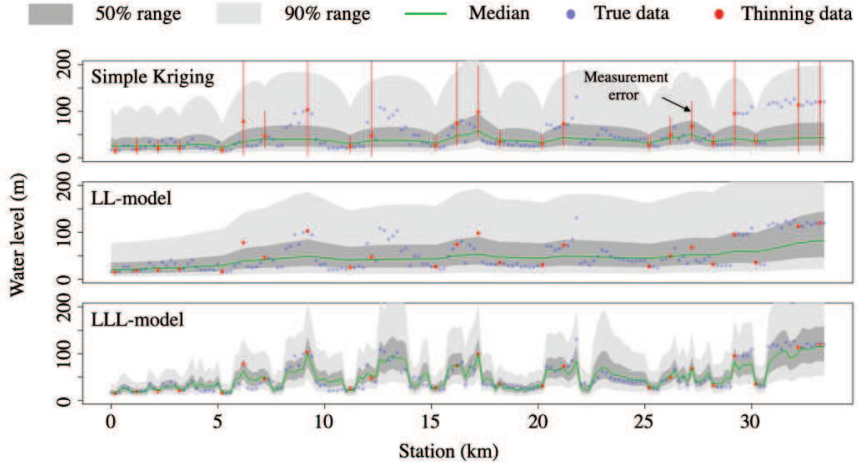

Figure 3. Estimation result of critical water level in each model

Figure 3 shows the results of estimating the spatial distribution of critical water level by applying each model defined in Section 3.3 to the thinning data. The thinning data is indicated by a red dot in the figure 3 and it is approximately 1km away between thinning data. From the upper part shows the results of the Simple Kriging, LL-model and LLL-model respectively. The light-gray and dark-gray shaded areas are the predicted sections for 50% and 90%, respectively, and the green line is the median of critical water levels h_c (m). In the Simple Kriging and LL-model, the critical water level h_c (m) changes smoothly, and the interpolation error between thinning data is large. On the other hand, in the LLL-model, the trend is more complicated and the interpolation error between thinning data is smaller than the other models.

Figure 4 shows a box plot of the state noise, observation noise, and regression coefficients which are the unknown parameters in the LL-model and LLL-model. In the local levee condition, in particular, the sensitivity of $z_{i,4}$ which is the variations of medium and small scale flooding in the past is large.

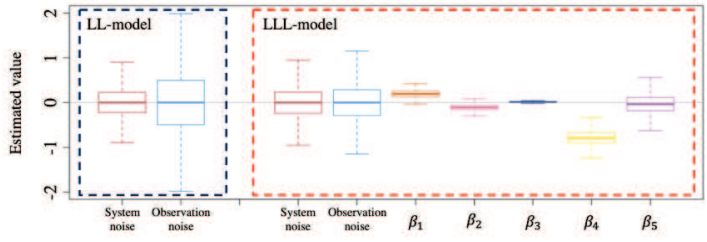

Figure 4. Box plot of the parameters estimated by state-space model

5 Final Remarks

This study estimated the spatial distribution of the critical water level h_c (m) for piping from discrete observations using three different models. Based on the results of spatial distribution of the piping hazard, interpolation of non-investigation points is possible with three models, but the interpolation error of LLL model is especially small, and correct data is interpolated effectively. By modeling continuously observable information such as "local levee condition", it is possible to further quantify potential fluctuations, and examining its sensitivity can be important information in decision making. Further, the authors will attempt to more appropriately clarify the influences between the interpolation error of each models and the number of investigations, and extend the results in this study to realization of risk informed decision making.

References

Durbin, J. and Koopman, S.J. (2002). A simple and efficient simulation smoother for state space time series analysis. *Biometrika*, 89(3), 603–615.

Durbin, J. and Koopman, S.J. (2012). *Time Series Analysis by State Space Methods, 2nd edition*, Oxford University Press, Oxford.

Fukaya, K. (2016). Time series analysis by state space models and its application in ecology. *Japanese Journal of Ecology,* 66, 375-389.

Higuti, T., Ueno, G., Nakano, S., Nakamura, K., and Yoshida, R. (2011). *Introduction to Data Assimilation-Next Generation Simulation Technology*, Asakura Publishing Co., Tokyo.

Hoshiya, M. and Yoshida, I. (1996). Identification of conditional stochastic Gaussian field, *Journal of Engineering Mechanics*, ASCE, 122(2), 101-108.

Matheron, G. (1973). Principle of geostatistics. *Economic Geology*, 58, 1246-1266.

Schweckendiek, T. (2014). *On Reducing Piping Uncertainties: A Bayesian Decision Approach*, TU Delft.

Shibata, R. (2017). *Time Series Analysis*, Kyoritsu Shuppan Co., Tokyo.